Astron. Astrophys. 316, 528–537 (1996)

ASTRONOMY
AND
ASTROPHYSICS

Latitude variations of ~ 7 MeV and > 300 MeV cosmic ray electron fluxes in the heliosphere: Ulysses COSPIN/KET results and implications

P. Ferrando[1], A. Raviart[1], L.J. Haasbroek[2], M.S. Potgieter[2], W. Dröge[3], B. Heber[3], H. Kunow[3], R. Müller-Mellin[3], H. Sierks[3], G. Wibberenz[3], and C.Paizis[4]

[1] CEA, DSM/DAPNIA/Service d'Astrophysique, CE-Saclay, F-91191 Gif-sur-Yvette Cedex, France
[2] Space Research Unit, Potchefstroom University, 2520 Potchefstroom, South-Africa
[3] Institut für Kernphysik, Universität Kiel, D-24118 Kiel, Germany
[4] Istituto di Fisica Cosmica, Universitá di Milano, I-20133 Milano, Italy

Received 23 February 1996 / Accepted 19 April 1996

Abstract. The 160° latitude scan performed in less than one year between summer 1994 and summer 1995 by Ulysses allowed us to obtain unique data about the latitudinal dependence of the cosmic ray fluxes. We present in this paper results on the electron component derived from the COSPIN/KET instrument onboard Ulysses, both at MeV and GeV energies.

The variations of the 1 to 7 GV electron fluxes do not show any feature which could be attributed to a latitude dependence. This observation deviates from the variations of the proton fluxes of similar rigidities. The electron/proton ratio is shown to depend unambiguously on latitude during the fast latitude scan of Ulysses. This latitudinal dependence can in fact be traced back in our data to at least mid 1993 when Ulysses left the streamer belt region.

The time profiles of high energy electrons and protons are also compared with the predictions of a time dependent modulation model. It is found that our data can be reasonably well accounted for by assuming time-dependent increasing drift effects, asymmetric perpendicular diffusion and a rigidity (P) dependence for the parallel mean free path derived by Bieber et al. (1994), i.e. $\propto P^{0.3}$ between 0.9 and 2.5 GV.

Regarding the ~ 7 MeV electrons, we do not see any flux excess at the poles. This is in contradiction with the claim made by Simnett et al. (1995) of an entry of MeV galactic electrons over the poles. The flux excess they claim to have detected is inconsistent with our electron data by 30 to 60 standard deviations, depending on the spectral shape. We argue that this inconsistency may be attributed to a proton induced background in the Simnett et al. data. The KET data imply a conservative upper limit of 3.2 elec/m^2.s.sr.MeV for the galactic electron flux at this energy.

Key words: cosmic rays – Sun: activity – interplanetary medium

Send offprint requests to: P. Ferrando

1. Introduction

Although the basic physical processes describing the solar modulation of cosmic ray spectra have been known for more than 30 years (e.g. Axford 1965), the cosmic ray data are still not quantitatively explained (e.g. Potgieter 1994). Particularly debated is the importance of the gradient and curvature drifts on the particle propagation in the interplanetary magnetic field with respect to other processes playing a role in solar modulation, such as diffusion and/or the effects of global merged interaction regions present in the heliosphere (e.g. McDonald et al. 1993). The key feature of models in which drift effects play an important role is that the drift directions are opposite for oppositely charged particles. In this current cycle, with a $A > 0$ solar magnetic field, the proton drift is from the polar regions of the heliosphere to the heliospheric neutral sheet, whereas this is the opposite for electrons (e.g. Jokipii & Thomas 1981). Because of this, "drift" models predict for this cycle i) a clear positive latitude gradient for protons, and ii) a different latitude dependence for electrons compared to protons, which is moreover depending on the heliocentric distance.

Prior to the Ulysses measurements, the understanding of modulation, and the development of models, was based on data gathered at latitudes less than $\sim 30°$, both for the cosmic ray flux and for the solar wind and magnetic field parameters relevant to solar modulation. Although it has been possible to observe some evidence of a charge sign dependence of solar modulation based on in-ecliptic data (e.g. Garcia-Munoz et al. 1986, Tuska 1990, Tuska et al. 1991, Evenson et al. 1991, 1995), the signature of such an effect is clearly expected to be the largest at very high latitudes, which have been explored by Ulysses.

Ulysses was launched in October 1990, heading towards Jupiter for a gravity assist manoeuver which put it on a trajectory almost perpendicular to the ecliptic plane. It took then more than 2.5 years for Ulysses to reach the highest southern latitude,

80.2°, on September 13, 1994, at a heliocentric distance of 2.3 AU. Then Ulysses went down rapidly to the heliographic equator (reached on March 4, 1995, at 1.3 AU from the Sun) and climbed to the highest northern latitude, 80.2°, reached on July 31, 1995, at 2.0 AU from the Sun. For simplicity, the maximum southern (resp. northern) latitude will be referred to as the South (resp. North) Pole.

The period between the South and North Poles has two characteristics which are important for modulation studies. First, Ulysses distance to the Sun varied only between 1.3 and 2.3 AU during this period, whereas it varied by more than 3 AU during the slow climb in latitude between Jupiter and the South Pole; this minimizes the importance of radial gradient effects in the cosmic ray flux. Second, it was short, less than 11 months relative to the 11 years periodicity of the solar activity, and happened close to solar minimum; this minimizes the effects of temporal variations in the cosmic ray flux related to the change of solar activity. These two factors make the Ulysses 160° fast latitude scan a unique occasion to catch a "snapshot" of the cosmic ray flux as a function of latitude during a solar minimum activity period.

We present in this paper an analysis of the electron data collected during this fast latitude scan by the Kiel Electron Telescope (KET). The analysis of the KET proton data are given in the accompanying paper in this issue (Heber et al. 1996b). The data used consist of electron fluxes in the 4-12 MeV range and above $\sim$ 300 MeV. The low energy data have been presented from launch in late 1990 to mid 1993 in relation with the problem of the propagation of Jovian electrons (Ferrando et al. 1991, 1993a, 1993b, Rastoin et al. 1993, 1996a). This is the first time we discuss these data in relation with the study of the galactic electron modulation. The high energy results are a follow-up of the electron analysis presented in Rastoin et al. (1996b) for the period from launch to the South Pole, and have been partially presented in Ferrando et al. (1995). As in these previous papers, the electron flux will be compared to the proton flux at the same rigidity, also measured by the KET.

This paper is organized as follows : a brief description of the instrument is given in Sect. 2, with an emphasis on the low energy electron detection and background. We give in Sect. 3 the results concerning the $\sim$ 7 MeV electrons, with an upper limit of their flux, and the pole to pole variations. We also show in Sect. 3 that there is no "entry of galactic electrons into the high latitude heliosphere" as claimed in a recent paper by Simnett et al. (1995), and we argue that the Simnett et al. result might have been due to a proton induced background not correctly taken into account. Sect. 4 is devoted to the high energies, with results on particle fluxes and electron/proton ratio variations. In Sect. 5 we show that our high energy data can be reasonably well accounted for by a time-dependent modulation model which we discuss in some detail.

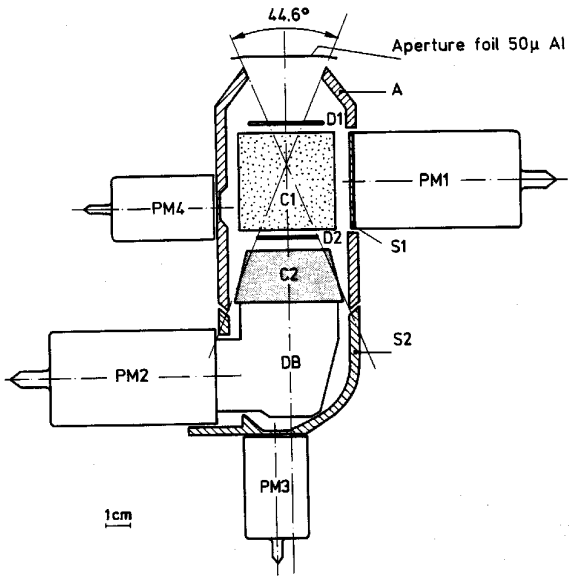

Fig. 1. Cross section of the KET instrument.

2. Instrumentation and data analysis

2.1. Instrument overview and detection efficiency

The KET electron telescope is part of the Ulysses cosmic ray and solar particle instrumentation (COSPIN) experiment, which has been described in detail in Simpson et al. (1992). The KET is designed to measure electron, proton, and alpha particle fluxes in several energy windows above a few MeV/n.

Functionally, the detector system (Fig. 1) consists of two parts : an entrance telescope and a calorimeter, both surrounded by a guard counter. The former is composed of a silica-aerogel Cerenkov detector C1 inserted between two semi-conductor detectors, D1 and D2. Together with the guard counter A, this combination defines the geometry, selects particles with velocity $\beta > 0.938$ and determines the particle charge. The calorimeter C2 consists of a 2.5 radiation length lead-fluoride (PbF2) crystal used as Cerenkov detector, in which electron showers develop. Finally, the scintillator S2 detects events not absorbed in C2.

Three electron channels are defined according to the detector responses, with the common requirement that a Cerenkov signal is seen in C1, and that no particles trigger the anticoincidence. The lowest energy channel, E4, corresponds to electrons entering D1 and stopping either in D2 or the top of C2 (no signal in C2 and S2); they have energies in the 4-12 MeV range. Data of this channel have been used in the analysis of Jovian electrons (Ferrando et al. 1993b, Rastoin et al. 1996a). The middle energy channel, E12, corresponds to electrons developing a sizeable shower in C2 with no charged particle detected in S2; the energy range of this channel is about 8-110 MeV. Electrons for which charged particles escape C2 and trigger S2 are counted either in the high energy proton channel (P4000) or in the highest energy electron channel (E300) depending on the amplitude of the C2 signal. For all these electron channels lower and upper thresholds are set in D1 and D2 at $\sim$ 0.4 and 3 times

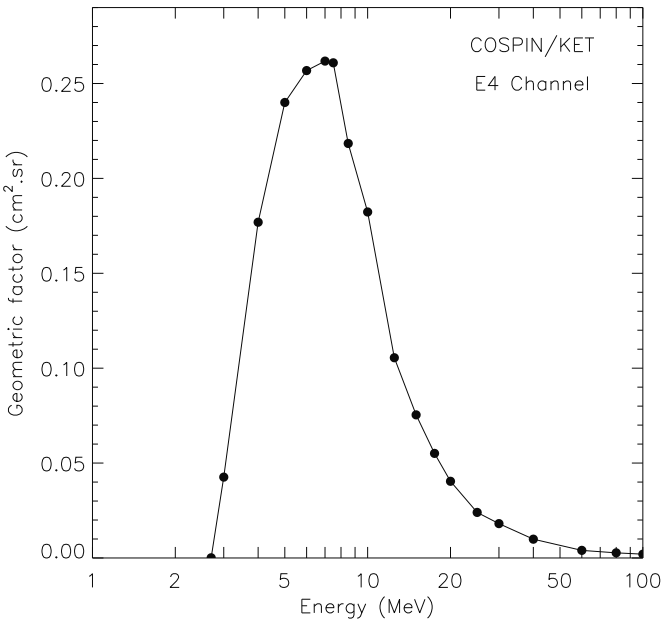

Fig. 2. Geometric factor of the E4 electron channel.

respectively the signal of a singly charged minimum ionizing particle.

The full analysis of the high energy electrons (E300) has been described in Rastoin et al. (1996b) and will not be repeated here. For completeness, we simply mention that it is based on a bidimensional analysis of the C2 and S2 response, which allows to i) distinguish electrons from protons, and ii) perform an energy selection for electrons. We have separated the electron data in 4 energy bands with averages of 0.9, 2.5, 3, and 7 GeV. We discuss below in more detail the low energy electron channels.

The E4 and E12 channels are nominally responding to particles entering the telescope through the aperture foil ("forward" particles). The requirement that these particles give a signal in the C1 Cerenkov and do not trigger the S2 penetration counter rejects all particles but electrons, since protons and alphas triggering C1 have a minimum energy of about 2 GeV/n, well above the one required for the complete traversal of all KET detectors ($\sim$ 130 MeV/n). These channels are thus pure electron channels as far as forward particles are concerned. Fig. 2 gives the efficient geometry factor G of the E4 channel as a function of energy, for an isotropic electron flux. It was derived from extensive calibrations with electron beams, complemented by detailed Monte-Carlo simulations (see Simpson et al. 1992). G has a maximum value G_{max} of 0.26 cm^{2}sr at 7 MeV, and FWHM energy limits of 3.7-11.7 MeV.

Together with that of the E12 channel, this E4 efficiency was used to derive the electron spectrum below 25 MeV during flux enhancements due to Jovian electron events, when Ulysses was still close to the Earth (Ferrando et al. 1991). The spectrum was found to be entirely consistent with measurements from other experiments. This is an independent check of the correctness of our determination of the E4 and E12 geometry factors.

Although these channels are completely insensitive to direct proton and alpha particles, they respond to other types of background. We have identified two of importance, both of them due to gamma rays entering KET without being flagged by the anticoincidence A or the penetration detector S2 : i) low energy gamma rays generated by the Ulysses RTG, and ii) gamma rays generated by cosmic ray interactions with the spacecraft. The former will be referred to as the "RTG" background, the latter as the "cosmic" background.

2.2. RTG background

The RTG background is due to gamma rays generated in the RTG, with energy less than $\sim$ 7 MeV, which are either converted into an electron-positron pair or give rise to photoelectric or Compton electrons inside KET. Only the E4 channel is contaminated by this background. Its level was measured in two occasions during RTG tests on ground, and was found to be $\sim 3 \times 10^{-3}$ c/s. The lowest count rate observed in the E4 channel during the flight is $\sim 2 \times 10^{-3}$ c/s, much less than the RTG ground test count rate. This is because the latter included events due to gamma rays generated (by the RTG radiation) in the walls of and in the material inside the test room. It is very difficult to determine the part due to the RTG background in the flight data. A tentative estimate, based on a model dependent analysis of the C2 pulse height distribution shape, gives $\sim 10^{-3}$ c/s.

Although the time dependence of the RTG background in the E4 channel cannot be estimated, it is probably weak as shows the evolution of the single detector count rate of D2, which integrates all events leaving more than 185 keV in this detector. The RTG induced counts in D2 are found by subtracting from the raw D2 rate the part due to real cosmic rays measured in the coincidence channels. We found that the RTG counts in D2 increase steadily with time, at a rate of $\sim$ 3.5 % per year. As noted above, this measurement is by no means the evolution of the RTG background in the E4 coincidence channel. As a matter of fact, the lowest E4 count rate observed in 1995 (See Fig. 4) is at the same level as the lowest count rate observed mid 91 during a period in which the Jovian electron flux was minimum.

2.3. Cosmic background

The cosmic background affects both the E4 and E12 channels. It consists of gamma rays created via interaction of high energy cosmic ray protons with the spacecraft body. These gamma rays enter backwards into KET through S2 without triggering it. They then convert into an electron-positron pair in the C2 calorimeter, which, depending on the depth of the conversion can lead to the development of an electromagnetic shower. A large part of these events are rejected by the coincidence requirement, either because one electron escaping C2 is striking the anticoincidence A, or because they generate more than two particles in the D1-C1-D2 system (rejection by upper thresholding of D1 and D2). However, for a fraction of these gamma ray events, only one or two electrons are going out of C2 and into the right geometry, so that valid signals in D2, C1, and D1 are generated. They are

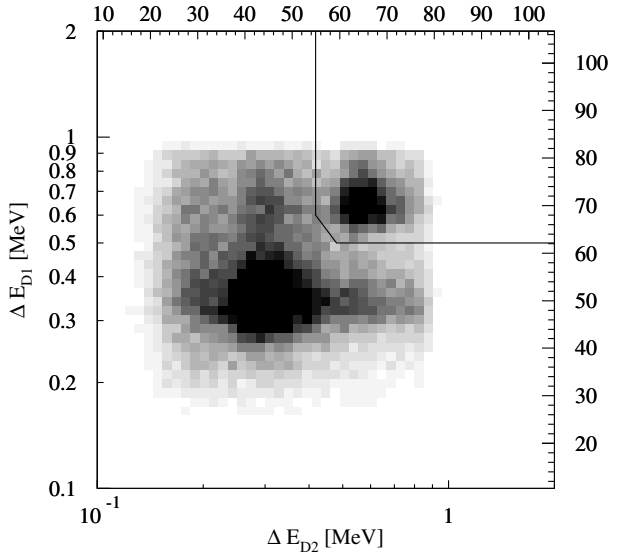

Fig. 3. D1-D2 PHA distribution for E4 events. The axis are labelled in channels and in the corresponding energy losses. The peaks are located at one and two times the signals for a singly charged minimum ionizing particle. The heavy line marks the selection chosen between $E4_{1el}$ and $E4_{2el}$ events.

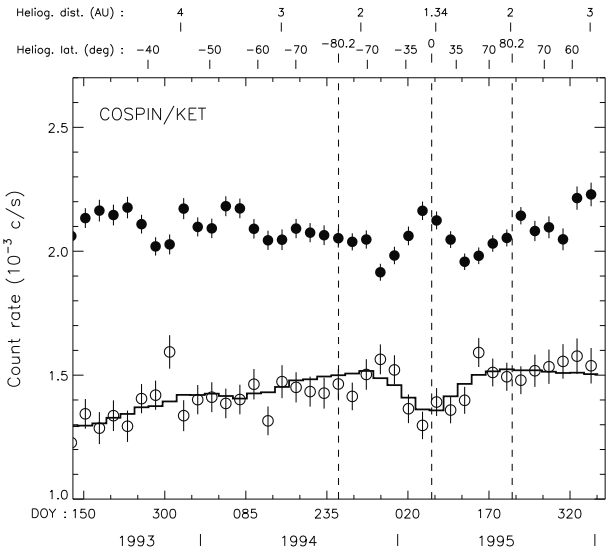

Fig. 4. 26-day averaged count rates of : $E4_{1el}$ events (•), $E4_{2el}$ events times 4 (○), and arbitrary normalized high energy protons (P4000 channel, histogram). The vertical lines indicate the passages at the poles and at the heliographic equator.

thus detected as E4 or E12 events, depending on the size of the C2 pulse.

We do have a direct measurement of gamma ray induced events which give 2 electrons in the D1-C1-D2 system, as illustrated in Fig. 3. This figure displays the D1-D2 distribution for E4 events accumulated from mid 93 to end of 95 (a similar distribution is obtained with E12 data). There is a main peak located at channel numbers 48 and 45 in D1 and D2 respectively, corresponding to a singly charged minimum ionizing particle. A second peak occurs at D1 = 70, D2 = 66, and exactly corresponds to two singly charged minimum ionizing particles, as can be seen on the energy scale indicated in the figure. The heavy line around this second peak is the limit set for the selection of "1 electron" and "2 electron" events, which will be referred to as $E4_{1el}$ and $E4_{2el}$, respectively, in this paper. The $E4_{2el}$ events represent $\sim$ 15 % of the total number of E4 events in these data. As expected because of the nature of the $E4_{2el}$ events, their fraction was much less during interplanetary flux increases due to Jovian electrons, and went down to $\sim$ 0 % during the traversal of the Jovian magnetosphere. The C1 Cerenkov response of the $E4_{2el}$ events was found to be twice that of the $E4_{1el}$ events, proving that both particles in the $E4_{2el}$ events are indeed relativistic. This fully confirms that we are dealing with a pair of electrons created by a gamma ray conversion in KET, mainly in the thick C2 detector.

Fig. 4 shows the time profile of the 26-day averages of the count rates of the 1 and 2 electron E4 events, since mid 1993 when Ulysses was out of the streamer belt region and up to the very beginning of 1996. The $E4_{2el}$ count rate (open circles) has been multiplied by a factor of 4. In addition, we have plotted as a solid histogram the high energy proton ($>$ 2.35 GeV, see Rastoin et al. 1996b) P4000 channel count rate with an arbitrary normalization. It is clear that the $E4_{2el}$ and the P4000 rates track each other, with only 7 $E4_{2el}$ points out of 37 displayed differing by more than one standard deviation from the P4000 rate. Both rates increase with time and latitude up to the South Pole, then decrease down to the heliographic equator and increase again up to the North Pole. This correlation shows that most of the cosmic background is created by protons above a few GeV, close to the peak of the proton spectrum. The $E4_{1el}$ events count rate (closed circles) has a different time profile, which is discussed in the next section.

Whereas all $E4_{2el}$ events are clearly gamma ray generated events, and can easily be rejected for the analysis of galactic electrons, $E4_{1el}$ events are unfortunately not completely free of background. To reach a better understanding of the E12 channel, which should have been the main electron channel of KET, we have performed detailed Monte-Carlo simulations of gamma rays with various energies entering backwards into KET. We found that the majority of gamma rays with energy less than $\sim$ 300 MeV give rise to a 1 electron event in D1-C1-D2 in the E12 channel. As a matter of fact, most of the E12 channel (1 electron selected) count rate is due to this cosmic background, which prevents the use of this channel for the study of galactic cosmic rays. Although a detailed study was not performed for the E4 channel, we suspect that similarly to what happens for E12, a non-negligible part of the $E4_{1el}$ count rate is generated by the cosmic background.

3. Low energy results

3.1. Observations and upper limit on flux

The time profile of the 26-day averaged $E4_{1el}$ count rates shown in Fig. 4 has definitely a shape different from the cosmic background. From mid 1993 to the South Pole, it slightly decreases on average, oppositely to the $E4_{2el}$ evolution which exhibits an increase. During the fast latitude scan, the $E4_{1el}$ count rate has a minimum around 60° south and north and peaks close to the heliographic equator, also opposite to the $E4_{2el}$ evolution which has a minimum at the equator. It is then relatively constant or increasing.

As stated in Sect. 2.2, about half or more of the $E4_{1el}$ rate is due to the RTG background which has a monotonic time evolution. Another part of the $E4_{1el}$ rate is due to the cosmic background, which has a time profile similar to the P4000 and $E4_{2el}$ profiles. Clearly the $E4_{1el}$ rate profile cannot be reproduced by a combination of these two types of background, and must then include a sizeable fraction of "real" electrons.

If we concentrate on the fast latitude scan period, which is the cleanest for the reasons given in the introduction, we get a latitude dependence of the $E4_{1el}$ rate as plotted in Fig. 5. Taken at face value, there is a minimum in the flux around 60° for both hemispheres, significantly below the maximum latitude flux, and a maximum of flux in the equatorial regions. We note that the rise of the flux close to equatorial regions is expected due to the reappearance of Jovian electrons which are confined in these regions. The observed level is consistent with the minimum flux observed in 1991 during the worst magnetic connection to Jupiter, as well as the modeling of Jovian electrons propagation (Rastoin, 1995). If we assume that the equatorial flux increase is indeed due to Jovian electrons, then the galactic electron flux does present a minimum close to the equatorial regions. However, we note that this conclusion is not supported by the data before and after the fast latitude scan : prior to the South Pole and after the North Pole, there is an indication, if anything, of a flux decrease with latitude. In addition to that, there are two long duration increases around day 200 of 1993 and beginning of 1994 for which we have no simple explanation.

The situation is thus not clear for low energy electrons. It should also be kept in mind that our observations do include a time dependent factor that we cannot monitor, like for protons (e.g. Heber et al., 1996a, 1996b, Paizis et al. 1995), due to the lack of a 1 AU baseline. We will thus take a conservative approach, and conclude that there is no significant variation of the low energy electron flux with latitude.

From the $E4_{1el}$ count rate, we can get a solid upper limit on the electron flux at $\sim$ 7 MeV, in the E4 channel 4-12 MeV energy range. Using the E4 geometric factor curve (Fig. 2), assuming an RTG background of 10^{-3} c/s in E4, and considering the $E4_{1el}$ rate of about its minimum value (2×10^{-3} c/s), we get a flux measurement of 3.2 elec/m^2.s.sr.MeV for a flat spectrum, or $500\times$ E$^{-2.5}$ elec/m^2.s.sr.MeV for a power law spectrum with the energy E in MeV. This upper limit, valid for the whole period presented (mid 1993 to end of 1995), is displayed on Fig. 11 and will be discussed in Sect. 5.

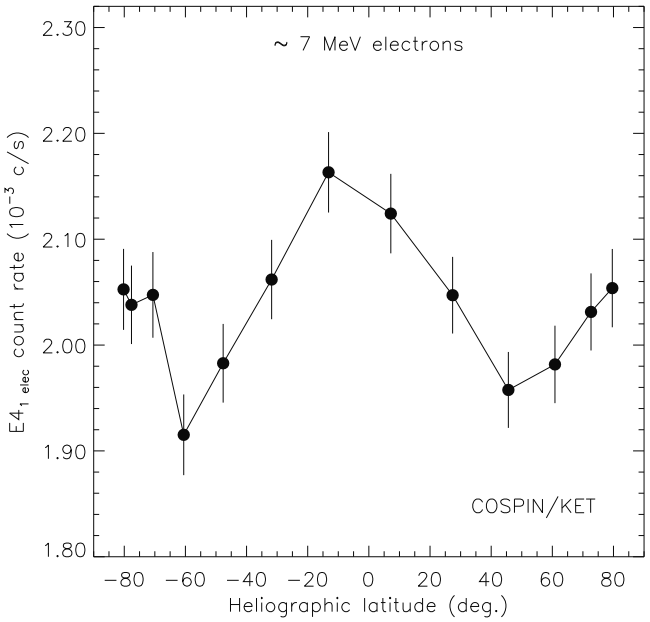

Fig. 5. 26-day averaged count rates of $E4_{1el}$ events during the fast latitude scan, as a function of heliographic latitude.

As we are not certain about the level of RTG and cosmic backgrounds, we conservatively consider this measurement as an upper limit in this paper. It is however clear from the above discussion that the $E4_{1el}$ events do include a large fraction of non-background events. We should be able to measure it in the future when we have performed a more quantitative study of the background in the E4 channel.

3.2. On the absence of a high latitude flux excess

In a recent paper, Simnett et al. (1995) argued to have observed with the HI-SCALE instrument onboard Ulysses an entry of galactic cosmic ray electrons over the solar poles. These electrons would be in the 1-20 MeV range, a range not covered by the nominal HI-SCALE channels. Their result was based on an analysis of the single detector background rate time profiles. They found a latitudinal integral flux excess of 320 elec/m^2.s.sr, which they converted into a differential flux excess for two spectral indices : $480\times$ E^{-2} and $1400\times$ E^{-3} elec/m^2.s.sr.MeV with E in MeV and considering only energies above 1.5 MeV.

This is in discrepancy with our measurements. By convolving the KET E4 geometric factor with such polar flux excess we found that the KET E4 channel count rate should have increased by 2.3×10^{-3} c/s (resp. 1.2×10^{-3} c/s) from equator to pole for the E^{-2} spectrum (resp. E^{-3} case), i.e. by an amount as large as the observed rate. This was not the case. As shown in Fig. 5 the statistical error on the $E4_{1el}$ rate is about 4×10^{-5} c/s. We thus should have seen the polar excess claimed by Simnett et al. (1995) with a significance of $\sim$ 60 standard deviations for the E^{-2} spectrum case ($\sim$ 30 σ for the E^{-3} case).

We are fully confident in our conclusion because it is based on the straightforward and comprehensive analysis of a triple

coincidence, fully calibrated, KET channel as opposed to the difficulties of the analysis of a single detector background rate performed by Simnett et al. Moreover, and as stated in Sect. 2, the validity of the E4 geometric factor was independently confirmed by the derivation of the Jovian electron spectrum.

We think that the excess claimed by Simnett et al. is simply due to the cosmic background, which was not correctly taken into account. They base their main conclusion on the F'C channel of the LEFS60 instrument. Inspecting their Fig. 2, one can see that the F'C rate has exactly the same average shape as the KET high energy P190 (0.28-2.35 GeV) and P4000 ($>$ 2.35 GeV) proton rates (see our Fig. 4 and 6), with a quantitative agreement for the relative importance of latitudinal versus temporal variations. In addition, one can find a one to one correspondence between the peaks of the F'C rate and the peaks of the P190 and P4000 rate in the daily averages; for example, the F'C rate increase around day 40 of 1995 is also present in our proton data (see Fig. 1 in Heber et al. 1996b). Consequently, the most natural explanation of the HI-SCALE F'C rate time profile is that this rate is completely dominated by cosmic background, as are the KET $E4_{2el}$ events and the KET E12 events (even when "1 electron" selected, as discussed in Sect. 2.3).

In short, the KET results discussed in the previous section rule out any significant excess of the galactic MeV electron flux over the poles, as claimed by Simnett et al. (1995) whose result might have been due to an underestimation of the cosmic background. On the opposite, the KET measurements rather show a slight excess of the total electron flux (galactic plus unknown fraction of Jovian) at the equator compared to the poles.

4. High energy results

We now turn to energies above $\sim$ 300 MeV, for which there exist no problems due to RTG or cosmic background. Rastoin et al. (1996b) presented the KET data up to the South Pole for four electron channels with average rigidities of 0.9, 2.5, 3 and 7 GV, in comparison with KET proton or alpha channels with similar rigidities. We will concentrate here on the fast latitude scan part, and drop the 3 GV electron channel which does not differ significantly from the 2.5 GV channel. Again, the reader is referred to Rastoin et al. (1996b) for all details about calibrations, proton rejection, detector gain monitoring, and energy analysis.

Fig. 6 shows 26-day averaged count rates of the 0.9, 2.5 and 7 GV electrons from mid 1993 up to the end of 1995. The data have been arbitrarily normalized. In the same figure we show the count rates of the KET proton channels with rigidities similar to those of the electrons. The proton data are displayed as a histogram, and have negligible statistical errors. Electron and proton rates are normalized at the South Pole. The 7 GV electron flux is rather constant within statistical uncertainties, and no significant feature relative to the 7 GV protons can be seen in our data. We will not discuss further this very high rigidity. The 0.9 and 2.5 GV electron and proton fluxes are steadily increasing

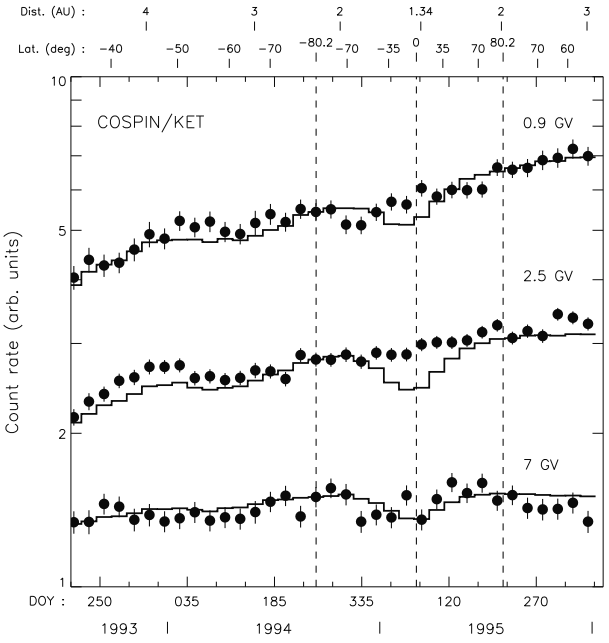

Fig. 6. Electron (•) and proton (histogram) count rates as a function of time, at 0.9, 2.5, 7 GV. The proton count rates are normalized to the electron ones at the South Pole. The vertical lines indicate the times when Ulysses was at the maxima of latitude, and in the heliographic equator.

with time, showing that the recovery, at least at high latitudes, is not completed at the end of 1995.

There are two important facts to be noticed when comparing electrons to protons. The first one is that the fluxes, which have been normalized at the South Pole, are also in agreement within errors at the North Pole. This suggests that the recovery of electrons and protons has the same time dependence during the 11 months separating South and North Pole passages. The second one is that there is a marked difference between the electron and proton time profiles during the fast latitude scan. The proton profiles have the typical shape due to the positive latitudinal gradient of these particles (Heber et al. 1996b), with a minimum of flux at the heliographic equator. On the opposite, the electron time profiles do not show any sign of latitudinal gradient, neither positive nor negative. This result, which appears to be present at 0.9 GV, is most significant at 2.5 GV.

We show in Fig. 7 the variation of the electron/proton ratio at 2.5 GV, obtained from the data of Fig. 6. The black dots with error bars are from the data taken during the fast latitude scan. The e/p ratio is normalized to unity at the South Pole. The open circles (error bars omitted) are from data taken before and after the fast latitude scan. This figure emphasizes the different variations with latitude of electron and proton rates. The e/p ratio varies by about 20 %. It is very clear from this figure that this latitude effect was present with the same level in the KET data since mid 1993, i.e. when Ulysses was above $\sim 40°$S.

The evidence of a latitude effect since mid 1993 seems to be in contradiction with our earlier claim of no latitude effect

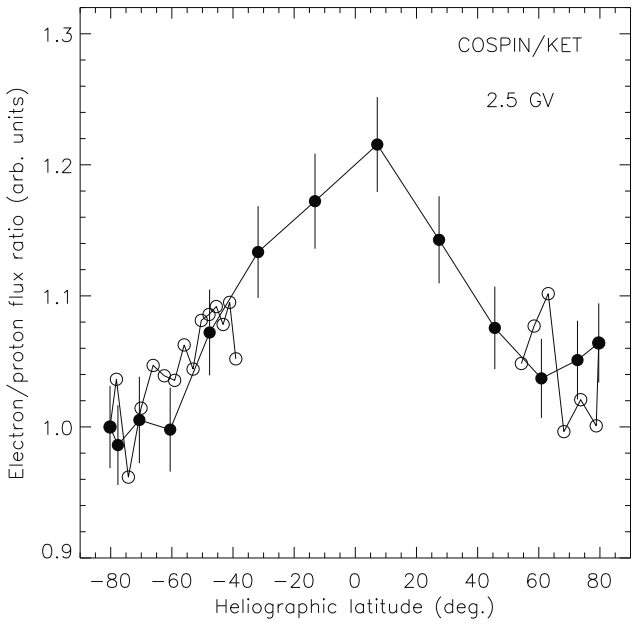

Fig. 7. Ratio of electron to proton count rates, at 2.5 GV, as a function of latitude. Measurements during the fast latitude scan are represented by closed circles, while open circles (error bars omitted) are measurements obtained before the South Pole and after the North Pole passages.

(for the e/p ratios) up to the South Pole (Rastoin et al. 1996b). This is due to the fact that in this previous paper, we did not consider the e/p variations seen when going to large latitudes as very significant, especially because they are much smaller than the e/p variations in 1991 (a factor of 1.6 at 2.5 GV) when Ulysses was close to the ecliptic. Clearly, the fast latitude scan has been very useful in assessing the extent of the e/p variations as a function of latitude only. With this knowledge, we could trace back the beginning of this latitude effect, which is starting around mid 1993. The e/p ratio for earlier times shows large variations which are difficult to interpret (see Fig. 13 in Rastoin et al. 1996b). They do not allow us to draw any firm conclusion about the exact time when the latitude effect indeed started, but we do not exclude that this could be as early as mid 1992.

5. Modulation model simulations

We used a *time-dependent* numerical modulation model adopted from Le Roux (1990) to qualitatively simulate the general trends observed in the KET 0.9 and 2.5 GV electron and proton data. Our aim was to make qualitative conclusions about the possible time dependence of certain modulation parameters, i.e. gradient and curvature drift, diffusion, etc. Since this simulation was done for opposite charge states *and* at different rigidities, conclusions about charge dependent modulation and the rigidity dependence of the mean free path were also possible.

Exploratory work, using a similar approach was done by Haasbroek et al. (1995a). They found that the recovery of cosmic rays during the period from 1991 to 1996 was essentially governed by gradually increasing drift effects and decreasing magnetic turbulence due to the declining level of solar activity. Comparing their results with KET data, Ferrando et al. (1995) showed that the model work lacked in two main areas, namely i) the too large simulated latitudinal effect during the Ulysses polar passes, and ii) the strong rigidity dependence between 0.9 and 2.5 GV (see also Simpson et al. 1995). For the present model simulation we tried to improve the previous work by adding more justifiable content to address the above mentioned "short-comings".

5.1. Model parameters

For the present study we used as a starting point the model parameters used and fully described in Haasbroek et al. (1995a). Additional concepts added to the ones used above are described next.

To address the first "short-coming", we added the concept of asymmetric diffusion perpendicular to the Heliospheric Magnetic Field (HMF). This phenomenon was reported from experimental work on Jovian electron propagation (e.g. Hamilton & Simpson 1979, Rastoin 1995, Rastoin et al. 1996a), and theoretical arguments (e.g. Jokipii & Kóta 1995). This approach implies that two different values for the diffusion perpendicular to the HMF exist, i.e. $(\kappa_\perp)_{rr}$ and $(\kappa_\perp)_{\theta\theta}$ where $(\kappa_\perp)_{rr}$ contributes to the effective radial diffusion $\kappa_{rr} = \kappa_\parallel \cos^2\psi + (\kappa_\perp)_{rr} \sin^2\psi$ with ψ the spiral angle. In previous modulation studies we assumed that the two perpendicular coefficients were equal. Jokipii & Kóta (1995) argued that $(\kappa_\perp)_{\theta\theta} > (\kappa_\perp)_{rr}$ due to large-scale transverse HMF fluctuations, especially at high latitudes. It should be noted that Hamilton & Simpson (1979) and Rastoin (1995) found the opposite, i.e. that $(\kappa_\perp)_{\theta\theta} < (\kappa_\perp)_{rr}$. However, their result was obtained from the study of MeV Jovian electrons observed at moderate latitudes, so that it might not apply to high energy particles away from the equatorial plane. We assumed here a value of $(\kappa_\perp)_{\theta\theta} = 3.6(\kappa_\perp)_{rr}$. Furthermore, we increased the absolute value of the above coefficients linearly in time by a factor of 1.5. This is interpreted as a simulation of decreasing turbulence due to decreasing solar activity. It is a method to reduce the strong latitudinal effect and charge dependence given by "standard" drift models in contrast to observations.

Next we addressed the second "short-coming". In previous studies the rigidity dependence of the mean free path was conveniently taken as $\propto P^{1.0}$ above 0.4 GV, where P denotes the rigidity. Here we introduce the dependence calculated for the parallel mean free path by Bieber et al. (1994) using the damping model of turbulence with slab geometry. This dependence gives a mean free path that increases $\propto P^{0.3}$ between 0.9 and 2.5 GV. The effect of this change in rigidity dependence, here also assumed for the perpendicular mean free path due to the absence of a coherent theory for the latter, will be demonstrated in the next section.

Other minor additions to our previous simulation was the inclusion of two small merged interaction region (MIR) type structures, in mid 1993 and the beginning of 1994, which were probably the cause of cosmic ray flux decreases at Earth and Ulysses at the mentioned times. In our code these MIRs were as-

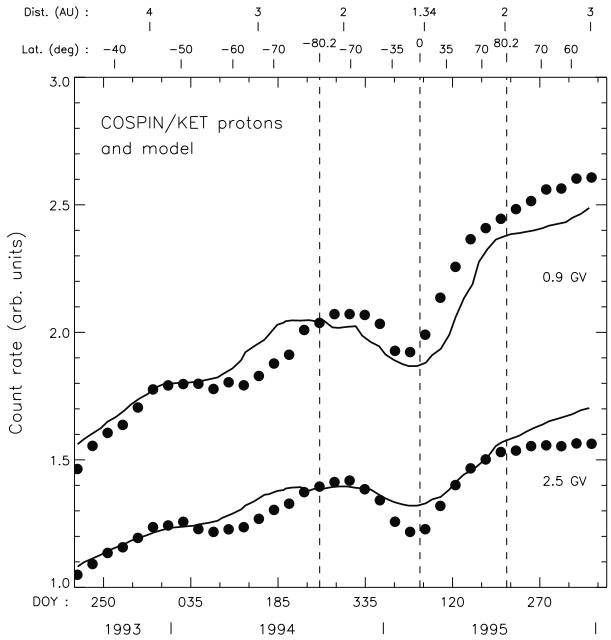

Fig. 8. Time-dependent modulation model results (lines) and proton fluxes (•) at 0.9 and 2.5 GV. Model and measurements are normalized at the South Pole. The vertical lines indicate the times when Ulysses was at the maxima of latitude, and in the heliographic equator.

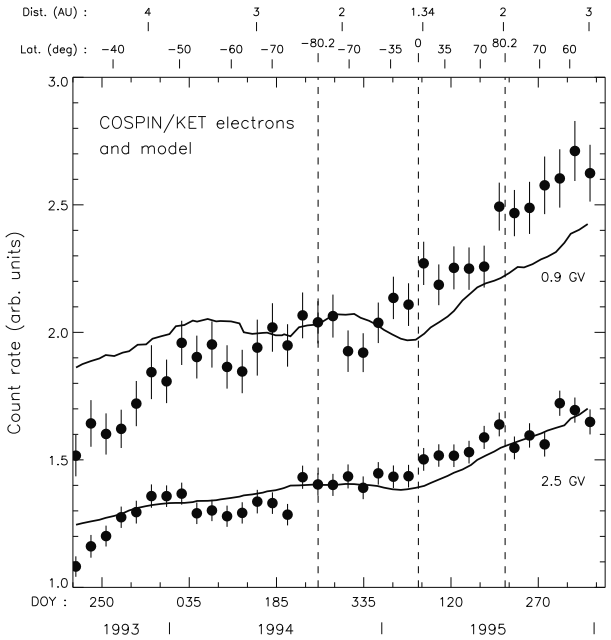

Fig. 9. Same as Fig. 8 for electrons.

sumed to be growing outward propagating regions of enhanced scattering, with a latitude extension of 45° from the equatorial plane. The values for the excursion of the heliospheric neutral sheet (HNS) above and below the equatorial plane, given by the "tilt angle" α, was provided by Hoeksema (1996). Similar to our previous simulation, global gradient and curvature drift effects were assumed to increase from a minimum in 1993 to a maximum at the end of 1995, to comply with the declining level of solar activity and value of α.

5.2. Comparison with high rigidity data

Figs. 8 and 9 show the model calculations (solid line) and the corresponding data. Notice that the general trends observed in the proton data, are also present in our simulation. In particular the 0.9 GV comparison for protons shows that the correct values for the latitudinal variation were obtained during the polar passes from mid 1994 to mid 1995. The model variation for 2.5 GV protons during the same period differs from the data by a factor of ~ 2. This indicates that the assumed rigidity dependence might still be too simple, although more acceptable than the $P^{1.0}$ assumption at high rigidities as discussed below. Regarding the electrons, the comparison of model with data shows that the order-of-magnitude increases are similar. The small-scale variations are due to the simulated MIR-type structures at the beginning of 1994. In general, the simulated increase with time during this period is due to the assumed decreasing turbulence and increasing drift effects.

Fig. 10 emphasizes the effect of the mean free path ($\lambda_{\parallel}$ and $\lambda_{\perp}$) rigidity dependence on the modelled fluxes. The data shown are the ratio of $\sim$ 0.9 to 2.5 GV protons, which increases with time, as expected since the modulation recovery is progressing. The full line is the result of the model described above, in particular with $\lambda_{\parallel}(P)$ and $\lambda_{\perp}(P) \propto P^{0.3}$ between 0.9 and 2.5 GV. The dashed line is obtained with the same parameters, except for the rigidity dependence of $\lambda_{\parallel}(P)$ and $\lambda_{\perp}(P)$ taken $\propto P^{1.0}$. One can notice the large difference between the two model curves, which shows the sensitivity of the model to the rigidity dependence of the mean free paths even in this restricted rigidity range. Although not perfect yet, the model with the Bieber et al. (1994) theoretical rigidity dependence is much closer to the data up to mid 1994, and then shows much more similar trends than does the model with the mean free paths $\propto P^{1.0}$. Finally, the dotted curve was obtained with the model we used in Ferrando et al. (1995). The comparison of this last curve with our present model does show the improvement resulting from the changes made in the parameters.

5.3. Comparison with low energy electron flux

Proton modulation is dominated by adiabatic energy changes below 300 MeV so that in diffusion-convection models the differential intensity is perfectly proportional to the kinetic energy of the protons. In drift models this spectral slope may change somewhat depending on which magnetic polarity cycle is considered. For this reason the averaged mean free paths for protons of these energies are "disguised" by adiabatic energy changes. Electrons on the other hand give a direct indication of the mean free path at these energies. Reliable observations of low energy electrons in the heliosphere can therefore assist greatly in

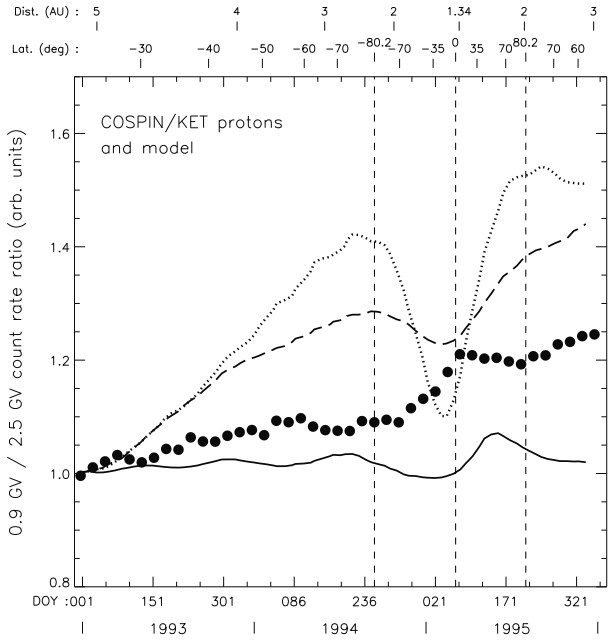

Fig. 10. 26-day averaged ratio of 0.9 GV to 2.5 GV proton count rates (•), compared to different models. *Full line* : model discussed in the text, in particular with the Bieber et al. (1994) rigidity dependence for the mean free path; *dashed line* : same model except for the parallel and perpendicular mean free path taken as $\propto P^{1.0}$; *dotted line* : model used in Ferrando et al. (1995). Data and model curves have been arbitrarily normalized to unity at the beginning of 1993.

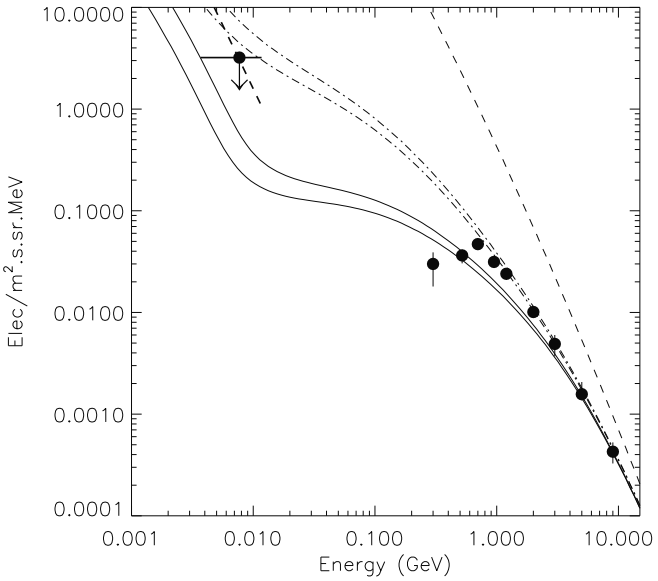

Fig. 11. KET measured electron spectrum versus time-dependent model prediction. The upper limit at $\sim$ 7 MeV, from this work, has been plotted assuming a flat spectrum (solid line) and a power law spectrum (index of -2.5, dashed line). The high energy data points are the KET spectrum measurement during the maximum of southern latitude in late 1994 (Rastoin et al. 1996b). The model spectra are shown for late 1994 (solid lines) and late 1995 (dashed-dotted lines); for each period the upper curve is calculated at 80° of helio-latitude, the lower curve at the heliographic equator. The assumed local interstellar spectrum is shown as the uppermost dashed line.

calculating mean free paths which on its part is essential for progress in modulation modelling. Now that the galactic interstellar electron spectrum is better known at these energies (Strong et al. 1994), electron observations can be useful in establishing which of the theoretical models for the parallel mean free paths given by Bieber et al. (1994) represents nature better. A detailed discussion of this topic is given by Potgieter (1996).

We simply mention here that the modelling discussed above, which was developed with the unique goal of qualitatively accounting for time and latitude variations, is not in strong contradiction with our upper limit on the flux at low energy. We compared in Fig. 11 the spectrum calculated in the above model to the KET spectrum measurements. The measured high energy flux corresponds to the maximum of southern latitude in fall 1994 (period D in Rastoin et al. 1996b), while the low energy upper limit is valid from (at least) mid 1993 up to the end of 1995. The model spectra are two "snapshots" taken from our long-term simulation, at the end of 1994 and end of 1995. For each model, we show the spectra calculated in the equatorial plane and at a latitude of 80°. It must be noted that the modelled electron flux, at this position in the very inner heliosphere, is larger at the poles than in equatorial regions. It is only at heliospheric distances larger than 10-20 AU that negative latitudinal gradients are expected to be present. This is described in detail in Haasbroek et al. (1995b).

In order to match the KET flux at high energy, we had to multiply the nominal interstellar spectrum by a factor of 2, which is certainly within the combined systematic uncertainties of the Strong et al. (1994) derivation and KET measurements. The spectrum calculated for late 1994 compares well with the measurements, although it should be possible to fine-tune the parameters to reach an even better agreement in the GeV region. The low-energy prediction for 1994 is well below our experimental limit. The evolution of the spectrum predicted by the model is the strongest around 20 MeV. The late 1995 calculated spectrum is higher than the KET upper limit at 7 MeV by a factor of $\sim$ 2 (80° curve). This discrepancy is not very large in view of the large sensitivity of electron fluxes to model parameters. It could probably be suppressed by assuming an energy dependence of the mean free path different from what we have taken. This is beyond the scope of this paper.

6. Summary and conclusions

In the present situation of cosmic ray experiments available in space, the fast latitude scan performed by Ulysses in 1994-1995 appears rather unique. It was almost complete with a 160° scan, within a small range of radial distance variation, and was fast during solar minimum conditions. This has allowed us to obtain, with the KET data, clean measurements of cosmic ray latitudinal properties in an almost steady-state heliosphere, both

for protons in Heber et al. (1996a, 1996b), and electrons in this paper.

In this work we have first shown that there is no entry of MeV electrons over the poles, contrary to the claim made by Simnett et al. (1995). We have measured a conservative upper limit on the electron flux in the 4-12 MeV range, that can be used to choose between the different models of parallel mean free paths at low energy. This upper limit should be lowered, or even changed to a solid measurement, once we have a better quantitative understanding of the backgrounds in the E4 KET channel.

On the high energy side, we have shown that electron and proton fluxes behave differently as a function of latitude. Electron fluxes do not show any sign of latitudinal dependence, on the contrary to protons. The effect is the strongest at 2.5 GV. The variation of the electron/proton ratio with latitude appears to be present in the KET data since at least mid 1993, when Ulysses was above 40°S. We have found however that these latitude variations are much smaller than the time variations observed close to the heliographic equator in 1991, during a maximum of solar activity.

We have finally compared our observations at 0.9 and 2.5 GV for protons and electrons with a comprehensive time dependent modulation model. We found that the observations can be well accounted for by the following realistic assumptions : i) global drift effects played an increasingly important role from 1993 to the end of 1995, ii) during this period the level of magnetic turbulence decreased, iii) generally, the diffusion perpendicular to the HMF is asymmetric with $(\kappa_\perp)_{\theta\theta} > (\kappa_\perp)_{rr}$, iv) the rigidity dependence of the parallel and perpendicular mean free path between 0.9 and 2.5 GV for protons and electrons is $\propto P^{0.3}$. Because of i) the charge dependence effects are becoming more and more visible with time in this model. In addition, the low energy electron fluxes computed with the same model were shown to reasonably agree with our experimental upper limit.

References

Axford W.I., 1965, Planet. Space Sci. 13, 115

Bieber J.W., Matthaeus W.H., Smith C.W., et al., 1994, ApJ 420, 294

Evenson P., Tuska E., Esposito J., Meyer P., 1991, Proc. of the 22nd Int. Cosmic Ray Conf. (Dublin) 3, 505

Evenson P., Huber D., Tuska-Patterson E., et al., 1995, J. Geophys. Res. 100, 7873

Ferrando P., Ducros R., Rastoin C., et al., 1991, Proc. of the 22th Int. Cosmic Ray Conf. (Dublin) 3, 366

Ferrando P., Ducros R., Rastoin C., et al., 1993a, Adv. Space Res. 13 (6), 107

Ferrando P., Ducros R., Rastoin C., Raviart A., 1993b, Planet. Space Sci. 41, 839

Ferrando P., Rastoin C., Raviart A., et al., 1995, Proc. of the 24th Int. Cosmic Ray Conf. (Rome) 4, 752

Garcia-Munoz M., Meyer P., Pyle K.R., Simpson J.A., 1986, J. Geophys. Res. 91, 2858

Haasbroek L.J., Potgieter M.S., Le Roux J.A., 1995a, Proc. of the 24th Int. Cosmic Ray Conf. (Rome) 4, 710

Haasbroek L.J., Potgieter M.S., Webber W.R., 1995b, Proc. of the 24th Int. Cosmic Ray Conf. (Rome) 4, 706

Hamilton D.C., Simpson J.A., 1979, ApJ 228, L123

Heber B., Dröge W., Kunow H., et al., 1996a, Geophys. Res. Lett., in press

Heber B., Dröge W., Ferrando P., et al., 1996b, A&A, this issue

Hoeksema, J.T., private communication, 1996

Jokipii J.R., Thomas B., 1981, ApJ 243, 1115

Jokipii, J.R., Kota J., 1995, Proc. of the 24th Int. Cosmic Ray Conf. (Rome) 4, 718

Le Roux, J.A., 1990, Ph.D. thesis, Potchefstroom University, South Africa

McDonald F.B., Lal N., McGuire R.E., 1993, J. Geophys. Res. 98, 1243

Paizis C., Heber B., Raviart A., et al., 1995, Proc. of the 24th Int. Cosmic Ray Conf. (Rome) 4, 756

Potgieter M.S., 1994, in : "Proc. of the 23rd Int. Cosmic Ray Conf. (Calgary), Invited, Rapporteur and Highlight Papers", Leahy, Hicks and Venkatesan Eds, World Scientific Publ. Cy, 213.

Potgieter M.S., 1996, J. Geophys. Res., submitted

Rastoin C., 1995, PhD thesis, Université de Paris VII

Rastoin C., Ducros R., Ferrando P., Raviart A., 1993, Proc. of the 23rd Int. Cosmic Ray Conf. (Calgary) 3, 346

Rastoin C., Ferrando P., Ducros R., et al., 1996a, J. Geophys. Res., submitted

Rastoin C., Ferrando P., Raviart A., et al., 1996b, A&A 307, 981

Simnett G.M., Tappin S.J., Roelof E.C., 1995, Geophys. Res. Lett. 22, 3341

Simpson J.A., Anglin J.D., Balogh A., et al., 1992, A&AS 92, 365

Simpson J.A., Connell J.J., Lopate C., et al., 1995, Geophys. Res. Lett. 22, 3337

Strong A.W., Bennett K., Bloemen H., et al., 1994, A&A 292, 82

Tuska E., 1990, PhD Thesis, Bartol University

Tuska E., Evenson P., Meyer P., 1991, ApJ 373, L27